Hindawi
Advances in High Energy Physics
Volume 2018, Article ID 7895967, 12 pages
https://doi.org/10.1155/2018/7895967

Research Article

Comparing Standard Distribution and Its Tsallis Form of Transverse Momenta in High Energy Collisions

Rui-Fang Si,[1,2] **Hui-Ling Li**,[3] **and Fu-Hu Liu**[1]

[1]*Institute of Theoretical Physics and State Key Laboratory of Quantum Optics and Quantum Optics Devices, Shanxi University, Taiyuan, Shanxi 030006, China*
[2]*Department of Mathematics and Science, Fenyang Normal Campus Lvliang College, Fenyang, Shanxi 032300, China*
[3]*Institute of Modern Physics, Shanxi Normal University, Linfen, Shanxi 041004, China*

Correspondence should be addressed to Hui-Ling Li; lihuilingxyx@sina.com and Fu-Hu Liu; fuhuliu@163.com

Received 26 October 2017; Accepted 2 January 2018; Published 19 March 2018

Academic Editor: Lorenzo Bianchini

 The publication of this article was funded by SCOAP[3].

The experimental (simulated) transverse momentum spectra of negatively charged pions produced at midrapidity in central nucleus-nucleus collisions at the Heavy-Ion Synchrotron (SIS), Relativistic Heavy-Ion Collider (RHIC), and Large Hadron Collider (LHC) energies obtained by different collaborations are selected by us to investigate, where a few simulated data are taken from the results of FOPI Collaboration which uses the IQMD transport code based on Quantum Molecular Dynamics. A two-component standard distribution and the Tsallis form of standard distribution are used to fit these data in the framework of a multisource thermal model. The excitation functions of main parameters in the two distributions are analyzed. In particular, the effective temperatures extracted from the two-component standard distribution and the Tsallis form of standard distribution are obtained, and the relation between the two types of effective temperatures is studied.

1. Introduction

High energy heavy-ion (nucleus-nucleus) collisions are an important method to simulate and study the big bang in the early universe, properties of new matter created in extreme conditions, accompanying phenomena in the creation, and physics mechanisms of the creation. Some models based on the quantum chromodynamics (QCD) and/or thermal and statistical methods can be used to analyze the equation of state (EoS) at finite temperature and density, properties of chemical and kinetic freeze-outs in collision process, distribution laws of different particles in final state, and universality of hadroproduction in different systems [1–5]. The properties of nuclear matter and its phase transition to quark-gluon plasma (QGP) at high temperature and density can be obtained. With the developments in the methodologies of experimental techniques and theoretical studies, the collision energy per nucleon pair in the center-of-mass system increases from high energy range which has a few to several hundred GeV to ultrahigh energy range which has presently a few to over ten TeV.

The temperature and density described the EoS showing that the new matter created in high and ultrahigh energy ranges is not similar to the ideal gas-like state of quarks and gluons expected by early theoretical models. Instead, the effects of strong dynamical coupling, long-range interactions, local memory, and others appear in the interior of interacting system. The rapid evolution of interacting system and the indirect measurements of some observable quantities result in that one can use the statistical method to study the distribution properties of some observable quantities such as (pseudo) rapidity, (transverse) momentum, (transverse) energy, azimuthal angle, elliptic flow, multiplicity, and others of final-state fragments and particles [1–5]. Thus, some quantitative or qualitative results related to the properties of interacting system and particle production can be observed.

As the quantities which can be early measured in experiments, that is, the so-called "the first day" measureable quantities, the rapidity and transverse momentum distributions attract wide attentions due to their carryovers on the information of longitudinal extension and transverse expansion of the

emission source in interacting system. With the increasing collision energy, the rapidity distribution range extends from a few rapidity units to over ten rapidity units, and the transverse momentum distribution range increases from 0 until a few GeV/c to 0 until over hundred GeV/c. Different functions and methods are used by different researchers to describe rapidity and transverse momentum distributions as well as other distributions which can be measured in experiments [1–5]. Based on a multisource thermal model [6–9], the rapidity and transverse momentum distributions obtained in experiments at different collision energies are studied by us in terms of two-cylinder, Rayleigh, Boltzmann, Tsallis, and other distributions. In particular, comparing with rapidity distribution, transverse momentum distribution contains more abundant information and attracts wider attentions. Although one has Monte Carlo and other indirect methods to describe transverse momentum distributions, analytical functions are more expected to use.

Because of the same transverse momentum distribution being described by different functions to obtain values of different parameters, possible relations existing among different parameters can be studied. In this paper, based on the multisource thermal model [6–9], the standard distribution (Boltzmann, Fermi-Dirac, and Bose-Einstein distributions) and its Tsallis form are used to describe the transverse momentum distribution of final-state particles produced in high energy nucleus-nucleus collisions. The excitation functions of effective temperatures obtained by the two distributions are extracted and the relation between the two effective temperatures is studied.

The rest part of this paper is structured as follows. A brief description of the model and method is presented in Section 2. Results on comparisons with experimental (simulated) data and discussion are given in Section 3. Finally, we summarize our main observations and conclusions in Section 4.

2. The Model and Method

According to the multisource model [6–9], a few emission sources of produced particles are assumed to form in interacting system due to different reaction mechanisms and/or data examples. For each emission source, the thermal model or other similar models and distributions can be used to perform calculation on the production of particles. The potential models include [10], but are not limited to, ideal gas-like model, ideal hydrodynamic model, and viscous hydrodynamic model. In these models, the relativistic effect has to be particularly considered, and the quantum effect can be usually neglected. If we study in detail the interacting system and final-state particles, both the relativistic and quantum effects have to be considered.

In the middle stage of collision process, the interacting system and emission sources in it can be regarded as to stay at the hydrodynamic state. After the stage of chemical freeze-out, in particular after the stage of kinetic freeze-out, the interacting system and emission sources in it should stay at the gas-like state. Otherwise, it is difficult to understand the kinetic information of singular particle measured in experiments. What had happened during the phase transition from the liquid-like state at the middle stage to the gas-like state at the final stage and why is beyond the focus of the present work. We shall not discuss this issue here.

According to the ideal gas model with the relativistic and quantum effects, the particle spectra can be described by the standard distribution. The number of particles is [11]

$$N = \frac{gV}{(2\pi)^3} \int d^3p \left[\exp\left(\pm \frac{E-\mu}{T_S} \right) + S \right]^{-1}, \quad (1)$$

where g is the degeneracy factor, V is the volume, p is the momentum, $E = \sqrt{p^2 + m_0^2}$ is the energy, m_0 is the rest mass, μ is the chemical potential, and T_S is the effective temperature; $S = 0$, $+1$, and -1 correspond to the Boltzmann, Fermi-Dirac, and Bose-Einstein statistics, respectively; $E - \mu > 0$ corresponds to plus +, and $E - \mu \leq 0$ corresponds to minus −. The invariant momentum distribution of particles is

$$E\frac{d^3N}{dp^3} = \frac{gV}{(2\pi)^3} E \left[\exp\left(\pm \frac{E-\mu}{T_S} \right) + S \right]^{-1}. \quad (2)$$

The normalized probability density distribution of particle momenta can be written as

$$f_p(p) = \frac{1}{N}\frac{dN}{dp} = C_S p^2 \left[\exp\left(\pm \frac{\sqrt{p^2 + m_0^2} - \mu}{T_S} \right) + S \right]^{-1}, \quad (3)$$

where C_S is the normalized constant in the standard probability density distribution of momenta. It is related to the selection of parameters.

The normalized joint probability density distribution of particle rapidities and transverse momenta is

$$f_{y,p_T}(y, p_T) = \frac{1}{N}\frac{d^2N}{dy\, dp_T} = C_S p_T \sqrt{p_T^2 + m_0^2} \cosh y \cdot \left[\exp\left(\pm \frac{\sqrt{p_T^2 + m_0^2}\cosh y - \mu}{T_S} \right) + S \right]^{-1}, \quad (4)$$

where $\sqrt{p_T^2 + m_0^2}\cosh y - \mu > 0$ corresponds to plus + and $\sqrt{p_T^2 + m_0^2}\cosh y - \mu \leq 0$ corresponds to minus −. The normalized probability density distribution of particle rapidities is then written to be

$$f_y(y) = \frac{1}{N}\frac{dN}{dy} = C_S \cosh y \cdot \int_0^{p_{T\max}} p_T \sqrt{p_T^2 + m_0^2} \left[\exp\left(\pm \frac{\sqrt{p_T^2 + m_0^2}\cosh y - \mu}{T_S} \right) + S \right]^{-1} dp_T, \quad (5)$$

where $p_{T\max}$ denotes the maximum transverse momentum. This rapidity distribution is only for an emission source. In the case of considering multiple sources, we have to consider sources distribution in the rapidity space [2–4, 12–16]. This issue is beyond the focus of the present work, and we shall not discuss it anymore. The normalized probability density distribution of particle transverse momenta is written to be

$$f_{p_T}(p_T) = \frac{1}{N}\frac{dN}{dp_T} = C_S p_T \sqrt{p_T^2 + m_0^2} \int_{y_{\min}}^{y_{\max}} \cosh y \cdot \left[\exp\left(\pm \frac{\sqrt{p_T^2 + m_0^2}\cosh y - \mu}{T_S} \right) + S \right]^{-1} dy, \quad (6)$$

where $y_{\max}$ and $y_{\min}$ denote the maximum and minimum rapidities, respectively.

It should be noted that, in the above formulas, although the same symbol C_S is used to represent the normalized constants in different formulas, these constants may be different from each other. In the case of considering multisource emission, we have to use the multicomponent distribution to describe the transverse momentum distribution of final-state particles. If n_0 emission sources are considered, we have

$$f_{p_T}(p_T) = \frac{1}{N}\frac{dN}{dp_T} = \sum_{i=1}^{n_0} k_{Si} \cdot C_{Si} p_T \sqrt{p_T^2 + m_0^2} \int_{y_{\min}}^{y_{\max}} \cosh y \cdot \left[\exp\left(\pm \frac{\sqrt{p_T^2 + m_0^2}\cosh y - \mu}{T_{Si}} \right) + S \right]^{-1} dy, \quad (7)$$

where C_{Si} denotes the normalized constant for the ith component in n_0 components, k_{Si} denotes the contribution fraction of the ith component in final-state distribution, and T_{Si} denotes the effective temperature corresponding to the ith component. There are temperature fluctuations among different components. In the case of considering multisource emission, we have the effective temperature of interacting system as $T_S = \sum_i k_{Si} T_{Si}$. Generally, two or three emission sources are enough to describe the experimental data obtained in soft excitation process. That is, $i = 2$ or 3 in most cases.

If we consider the Tsallis form of standard distribution, the number of particles is [11, 17]

$$N = \frac{gV}{(2\pi)^3} \int d^3p \left\{ \left[1 \pm \frac{q-1}{T_T}(E-\mu) \right]^{\pm 1/(q-1)} + S \right\}^{-1}, \quad (8)$$

where q is an entropy index which characterizes the departing degree of the interacting system from the equilibrium state. Generally, we have $q > 1$; if $q = 1$, the system stays in the equilibrium state. T_T is the effective temperature. Other symbols have the same meanings as (1). The invariant momentum distribution of particles is

$$E\frac{d^3N}{dp^3} = \frac{gV}{(2\pi)^3} E \left\{ \left[1 \pm \frac{q-1}{T_T}(E-\mu) \right]^{\pm 1/(q-1)} + S \right\}^{-1}. \quad (9)$$

The normalized probability density distribution of particle momenta is

$$f_p(p) = \frac{1}{N}\frac{dN}{dp} = C_T p^2 \left\{ \left[1 \pm \frac{q-1}{T_T}\left(\sqrt{p^2 + m_0^2} - \mu \right) \right]^{\pm 1/(q-1)} + S \right\}^{-1}. \quad (10)$$

The normalized joint probability density distribution of particle rapidities and transverse momenta is

$$f_{y,p_T}(y, p_T) = \frac{1}{N}\frac{d^2N}{dy\,dp_T} = C_T p_T \sqrt{p_T^2 + m_0^2}\cosh y \cdot \left\{ \left[1 \pm \frac{q-1}{T_T}\left(\sqrt{p_T^2 + m_0^2}\cosh y - \mu \right) \right]^{\pm 1/(q-1)} + S \right\}^{-1}. \quad (11)$$

Then, the normalized probability density distribution of particle rapidities is

$$f_y(y) = \frac{1}{N}\frac{dN}{dy} = C_T \cosh y \int_0^{p_{T\max}} p_T \sqrt{p_T^2 + m_0^2} \left\{ \left[1 \pm \frac{q-1}{T_T}\left(\sqrt{p_T^2 + m_0^2}\cosh y - \mu \right) \right]^{\pm 1/(q-1)} + S \right\}^{-1} dp_T. \quad (12)$$

The normalized probability density distribution of particle transverse momenta is

$$f_{p_T}(p_T) = \frac{1}{N}\frac{dN}{dp_T} = C_T p_T \sqrt{p_T^2 + m_0^2} \int_{y_{\min}}^{y_{\max}} \cosh y \cdot \left\{ \left[1 \pm \frac{q-1}{T_T} \left(\sqrt{p_T^2 + m_0^2} \cosh y - \mu \right) \right]^{\pm 1/(q-1)} + S \right\}^{-1} dy. \quad (13)$$

In the above formulas, although the same symbol C_T is used to represent the normalized constants in different formulas, these constants may be different from each other. As discussed in [17], the Tsallis form has at least four types of function representations, though we choose only one that contains p_T after C_T and the index $1/(q-1)$. We do not need to consider a multisource for the Tsallis form due to it covering a two- or three-component standard distribution, and the two- or three-component standard distribution describes well the transverse momentum spectrum of particles produced in soft excitation process.

It should be noted again that the above multicomponent (two- or three-component) standard distribution and the Tsallis form of standard distribution can describe only the transverse momentum spectrum of particles produced in soft excitation process. The transverse momentum spectrum produced in soft excitation process covers a narrow range. For the transverse momentum spectrum covering a wide range, we have to consider the contribution of hard scattering process. According to the QCD calculus [18–20], we have an inverse power-law

$$f_H(p_T) = \frac{1}{N}\frac{dN}{dp_T} = A p_T \left(1 + \frac{p_T}{p_0} \right)^{-n} \quad (14)$$

to describe the transverse momentum spectrum produced in hard scattering process, where p_0 and n are free parameters and A is the normalized constant which is related to the free parameters. It is obvious that a two-component function is needed for a wide transverse momentum spectrum. The first component is the multicomponent (two- or three-component) standard distribution or Tsallis form which describes the soft process, and the second component is the inverse power-law which describes the hard process. The application of the inverse power-law is beyond the focus of the present work. We shall not discuss it anymore.

In the above discussions, to obtain chemical potential of a given particle, the chemical freeze-out temperature $T_{\rm ch}$ of the emission source is needed to know first of all. In the case of assuming the same chemical freeze-out moment, the emission source has the sole $T_{\rm ch}$. According to [21, 22], there is a relation among $T_{\rm ch}$, the yield n_1 and mass m_1 of the first particle, the yield n_2 and mass m_2 of the second particle, and the ratio $n_{12} = n_1/n_2$. We have

$$n_{12} = \frac{n_1}{n_2} = \frac{\exp(m_2/T_{\rm ch}) + S_2}{\exp(m_1/T_{\rm ch}) + S_1}, \quad (15)$$

where $S_1(S_2) = \pm 1$ denote fermion and boson, respectively. If the fermion and boson are not needed to distinguish each other, we have $S = 0$. This results in a simple expression for (15); that is, $n_{12} = n_1/n_2 \approx \exp(-m_1/T_{\rm ch})/\exp(-m_2/T_{\rm ch})$.

In the framework of a statistical thermal model of noninteracting gas particles with the assumption of standard Maxwell-Boltzmann statistics, there is an empirical expression for the chemical freeze-out temperature [23–26],

$$T_{\rm ch} = \frac{0.164}{1 + \exp\left[2.60 - \ln\left(\sqrt{s_{NN}}\right)/0.45\right]}, \quad (16)$$

where $\sqrt{s_{NN}}$ denotes the energy per nucleon pair in the center-of-mass system. Both the units of $T_{\rm ch}$ and $\sqrt{s_{NN}}$ are in GeV. The limiting value of $T_{\rm ch}$ is 0.164 GeV.

In the framework of a thermal model with standard distribution, the chemical potentials of some particles can be obtained from the ratios of negatively to positively charged particles. According to [27], we have

$$\frac{\overline{p}}{p} = \exp\left(-\frac{2\mu_p}{T_{\rm ch}}\right) \equiv k_p, \quad (17)$$

$$\frac{K^-}{K^+} = \exp\left(-\frac{2\mu_K}{T_{\rm ch}}\right) \equiv k_K, \quad (18)$$

$$\frac{\pi^-}{\pi^+} = \exp\left(-\frac{2\mu_\pi}{T_{\rm ch}}\right) \equiv k_\pi, \quad (19)$$

where the symbol of a given particle is used for its yield for the purpose of simplicity. Further, the chemical potentials of the mentioned particles are

$$\mu_p = -\frac{1}{2} T_{\rm ch} \cdot \ln\left(k_p\right), \quad (20)$$

$$\mu_K = -\frac{1}{2} T_{\rm ch} \cdot \ln\left(k_K\right), \quad (21)$$

$$\mu_\pi = -\frac{1}{2} T_{\rm ch} \cdot \ln\left(k_\pi\right). \quad (22)$$

Empirically, the chemical potential for baryon is [23–26]

$$\mu_B = \frac{1.303}{1 + 0.286\sqrt{s_{NN}}} \quad (23)$$

which is also obtained in the framework of a statistical thermal model of noninteracting gas particles with the assumption of standard Maxwell-Boltzmann statistics, where both the units of μ_B and $\sqrt{s_{NN}}$ are in GeV.

We would like to point out that (16) and (23) should be modified in the framework of generalized nonextensive statistics when we use the Tsallis form of standard distribution. At the same time, (17)–(22) should be generalized within an analysis with the Tsallis form. To modify (16)–(23) is beyond our focus and ability. We shall not discuss these modifications here. Instead, as an approximate treatment, we use $T_{\rm ch}$ and μ_π obtained within an analysis with the standard distribution as those within the Tsallis form. In fact, the absolute value of μ_π is very small, and its effect on the

transverse momentum spectra can be neglected. Therefore, this approximate treatment is acceptable.

It should be noted once more that, as mentioned in the above discussions, what we extract from the multicomponent standard distribution or the Tsallis form of standard distribution is the effective temperature, but not the real temperature of emission source. Generally, the transverse momentum spectrum contains both the contributions of thermal motion and flow effect. The real temperature is only a reflection of purely thermal motion, and the flow effect should not be included in it. As for the methods to obtain the real temperature by disengaging the contributions of thermal motion and flow effect, we can use the blast-wave model based on the Boltzmann distribution [28–30], the blast-wave model based on the Tsallis distribution [31], the improved Tsallis distribution [32, 33], some alternative methods [21, 29, 34–36], and others [37–40]. These methods themselves are beyond the focus of the present work. We shall not discuss them anymore.

3. Results and Discussion

The transverse momentum spectra of negatively charged pions produced in midrapidity range in $\sqrt{s_{NN}}$ = 2.24 and 2.52 GeV central gold-gold (Au-Au) collisions [41] measured (simulated) by the FOPI Collaboration at the Heavy-Ion Synchrotron (SIS), 11.5 [42], 62.4, 130, and 200 GeV central Au-Au collisions [29] measured by the STAR Collaboration at the Relativistic Heavy-Ion Collider (RHIC), 22.5 GeV central copper-copper (Cu-Cu) [43] and 200 GeV central Au-Au collisions [27] measured by the PHENIX Collaboration at the RHIC, and 2.76 TeV central lead-lead (Pb-Pb) collisions [44] measured by the ALICE Collaboration at the Large Hadron Collider (LHC) are selected to investigate. Among them, the results of FOPI Collaboration are given in Figure 1 with the simulated data (the last eight circles) of the IQMD transport code [45] which is based on Quantum Molecular Dynamics [46]. To avoid confusion, most results of the STAR Collaboration are given in Figure 2, and the results corresponding to 11.5 GeV are given in Figure 3. The results of PHENIX and ALICE Collaborations are given in Figures 3 and 4, respectively. In each figure, the symbols represent the experimental (simulated) data scaled by different amounts in some cases. The collision energy and type, centrality and midrapidity ranges, and scaled amount if not 1 are marked in the panel. The dashed and solid curves denote the results fitted by the two-component standard distribution and the Tsallis form of standard distribution. The values of parameters, χ^2, and degree of freedom (dof) are listed in Table 1 ordered by the energy from low to high. In particular, $T_S = k_{S1}T_{S1} + (1 - k_{S1})T_{S2}$ is the average weighted by the fractions of different components, μ_π is obtained by (16) and (22), and the values of k_π in (22) at different energies are obtained from [47]. As a preliminary result, the values of μ_π for the first and second standard distributions and the Tsallis form are assumed to be the same. In the fitting, the method of least square is used to obtain the best parameter values. One can see that the two-component standard distribution and the Tsallis form of standard distribution describe approximately

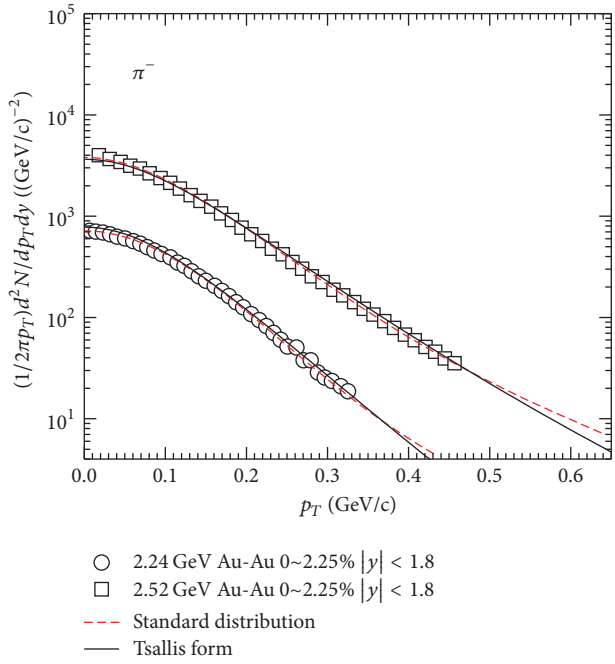

FIGURE 1: Transverse momentum spectra of π^- produced in central Au-Au collisions at $\sqrt{s_{NN}}$ = 2.24 (circles) and 2.52 GeV (squares). The symbols represent the experimental data of the FOPI Collaboration [41] measured in midrapidity range and the last eight circles represent the simulated data of the IQMD transport code [45] which is based on Quantum Molecular Dynamics [46]. The statistical errors are smaller than the size of symbols. The dashed and solid curves are the results fitted by the two-component standard distribution and the Tsallis form of standard distribution, respectively.

the transverse momentum spectra of negatively charged pions produced in central nucleus-nucleus collisions in the energy range from SIS to LHC.

To study the excitation functions of free parameters, that is, the dependence of free parameters on collision energy, the relations $T_{S1} - \ln\sqrt{s_{NN}}$ ($T_{S2} - \ln\sqrt{s_{NN}}$), $T_S - \ln\sqrt{s_{NN}}$ ($T_T - \ln\sqrt{s_{NN}}$), $k_{S1} - \ln\sqrt{s_{NN}}$, and $q - \ln\sqrt{s_{NN}}$ are presented in Figures 5–8, respectively. The symbols and error bars in the figures denote the values of free parameters and their errors. Both the values of free parameters and their errors are taken from Table 1. The lines in Figures 5 and 6 are obtained by the method of least square. These lines can be described by linear functions $T_{S1,S2,S,T} = a\ln\sqrt{s_{NN}} + b$, where the slope a and intercept b are listed in Table 1 and the unit of $\sqrt{s_{NN}}$ is in GeV. One can see that the four effective temperatures T_{S1}, T_{S2}, T_S, and T_T increase linearly with increase of $\ln\sqrt{s_{NN}}$. In particular, the relation between T_S and T_T can be obtained to be $T_S = (2.500 \pm 0.170)T_T + (-0.040 \pm 0.013)$ due to Table 1, which shows a linear relation between T_S and T_T. With increase of $\sqrt{s_{NN}}$, k_{S1} has a minimum at about 10 GeV, and q increases primitively and saturates at about 10 GeV.

Our results show some interesting features. Actually, one could as well say that there is no difference in the particle production in central nucleus-nucleus collisions from a few GeV to a few TeV. This in some sense echoes recent studies of

Table 1: Values of free parameters (T_{S1}, T_{S2}, and k_{S1}) for the two-component standard distribution, free parameters (T_T and q) for the Tsallis form of standard distribution, derivative parameters (T_S and μ_π), χ^2, and dof corresponding to the fits in Figures 1–4, as well as values of slope a and intercept b corresponding to the fits of linear functions $T_{S1,S2,S,T} = a \ln \sqrt{s_{NN}} + b$ in Figures 5 and 6. As a preliminary result, the values of μ_π for the first and second standard distribution and the Tsallis form are assumed to be the same. The units of effective temperatures and chemical potential are in GeV.

	T_{S1}	T_{S2}	k_{S1}	T_S	μ_π	χ^2/dof	T_T	q	χ^2/dof
2.24 GeV Au-Au (FOPI Collab.)	0.038 ± 0.004	0.100 ± 0.050	0.825 ± 0.100	0.049 ± 0.012	−(0.021 ± 0.002)	14.880/31	0.039 ± 0.005	1.042 ± 0.010	24.043/32
2.52 GeV Au-Au (FOPI Collab.)	0.054 ± 0.007	0.126 ± 0.012	0.810 ± 0.050	0.068 ± 0.008	−(0.019 ± 0.003)	11.004/42	0.040 ± 0.003	1.072 ± 0.008	16.856/43
11.5 GeV Au-Au (STAR Collab.)	0.076 ± 0.010	0.175 ± 0.009	0.432 ± 0.070	0.132 ± 0.009	−(0.005 ± 0.007)	1.350/18	0.067 ± 0.008	1.106 ± 0.008	2.850/19
22.5 GeV Cu-Cu (PHENIX Collab.)	0.088 ± 0.025	0.219 ± 0.008	0.620 ± 0.085	0.138 ± 0.019	−(0.003 ± 0.011)	4.123/19	0.075 ± 0.005	1.089 ± 0.004	1.360/20
62.4 GeV Au-Au (STAR Collab.)	0.106 ± 0.012	0.242 ± 0.029	0.620 ± 0.009	0.158 ± 0.019	−(0.002 ± 0.014)	2.130/6	0.070 ± 0.005	1.131 ± 0.011	1.561/7
130 GeV Au-Au (STAR Collab.)	0.102 ± 0.012	0.250 ± 0.060	0.600 ± 0.085	0.161 ± 0.031	−(0.001 ± 0.015)	6.246/6	0.076 ± 0.005	1.117 ± 0.016	42.448/7
200 GeV Au-Au (STAR Collab.)	0.112 ± 0.010	0.310 ± 0.085	0.671 ± 0.080	0.177 ± 0.035	−(0.002 ± 0.018)	10.241/7	0.078 ± 0.006	1.120 ± 0.015	10.736/8
200 GeV Au-Au (PHENIX Collab.)	0.134 ± 0.020	0.270 ± 0.010	0.761 ± 0.092	0.167 ± 0.018	−(0.002 ± 0.018)	3.048/24	0.089 ± 0.004	1.096 ± 0.005	7.650/25
2.76 TeV Pb-Pb (ALICE Collab.)	0.145 ± 0.010	0.345 ± 0.011	0.761 ± 0.040	0.193 ± 0.010	−(0.001 ± 0.011)	6.475/37	0.097 ± 0.005	1.112 ± 0.005	9.766/38
a	0.015 ± 0.012	0.034 ± 0.022		0.020 ± 0.023			0.008 ± 0.008		
b	0.035 ± 0.004	0.088 ± 0.007		0.067 ± 0.008			0.039 ± 0.003		

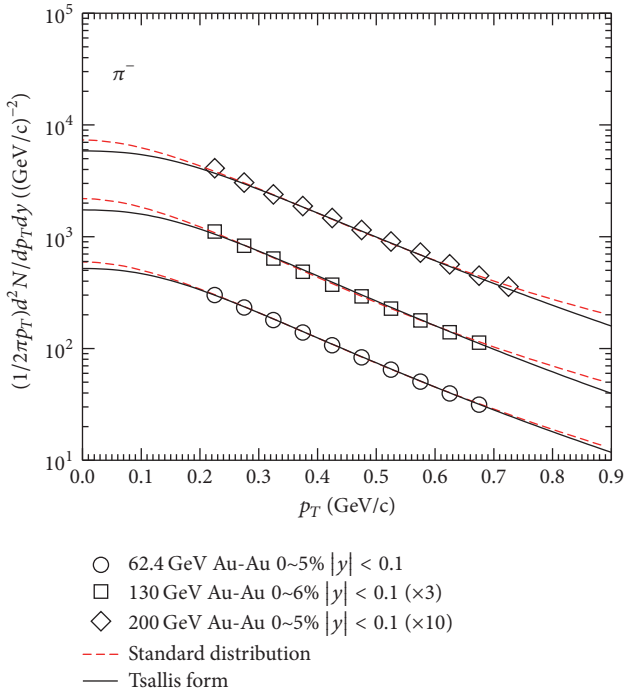

FIGURE 2: Same as Figure 1, but for $\sqrt{s_{NN}}$ = 62.4 (circles), 130 (squares), and 200 GeV (rhombuses). The symbols represent the experimental data of the STAR Collaboration with errors being the root quadratic sum of statistical and systematic errors [29].

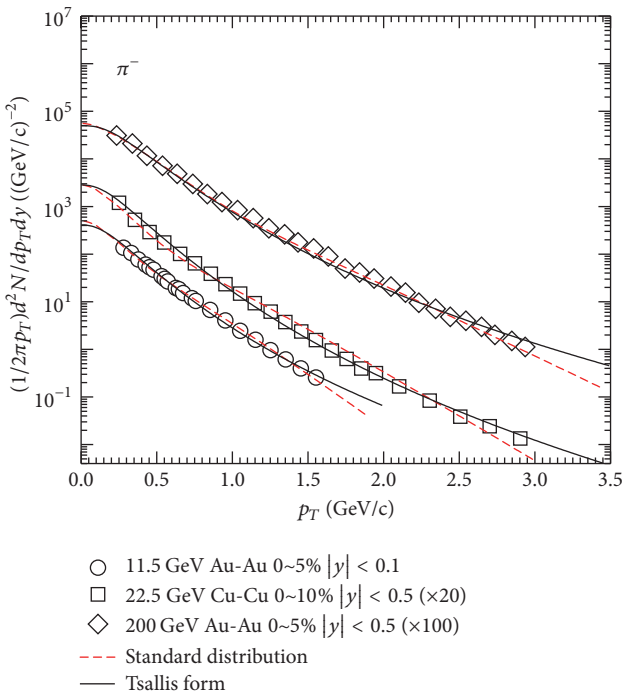

FIGURE 3: Same as Figure 1, but for central Au-Au collisions at $\sqrt{s_{NN}}$ = 11.5 GeV (circles), central Cu-Cu collisions at $\sqrt{s_{NN}}$ = 22.5 GeV (squares), and central Au-Au collisions at $\sqrt{s_{NN}}$ = 200 GeV (rhombuses). The symbols represent the experimental data of the STAR Collaboration with the statistical and systematic errors added in quadrature (circles) [42], and the PHENIX Collaborations with statistical errors only (squares [43] and rhombuses [27]).

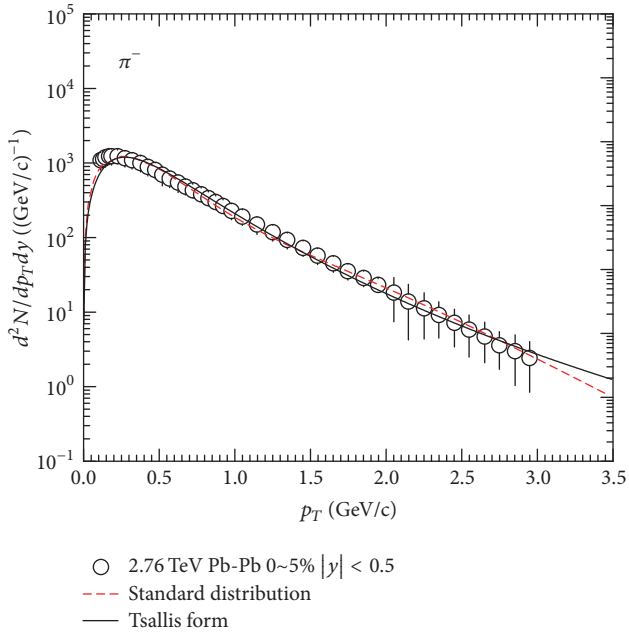

FIGURE 4: Same as Figure 1, but for central Pb-Pb collisions at $\sqrt{s_{NN}}$ = 2.76 TeV. The symbols represent the experimental data of the ALICE Collaborations and errors are the root quadratic sum of statistical and systematic errors [44].

Sarkisyan et al. [1, 48]. In addition, our recent study shows that the same or similar fits to be good for proton-proton collisions [40], though the parameter values in proton-proton collisions are closer to those in peripheral nucleus-nucleus collisions when comparing with central nucleus-nucleus collisions. This suggests universality in particle production, as it is obtained in recent and previous studies of Sarkisyan et al. [1, 12, 48–50], but now for transverse momentum distribution as well. On the other hand, the multiplicity and transverse momentum distributions observed in different data samples can be uniformly fitted by multicomponent Erlang distribution [8, 51, 52], which also show the universality in particle production. Indeed, the universality in particle production exists not only in mean multiplicity and pseudorapidity density but also in multiplicity and transverse momentum distributions in some conditions.

Our observation that k_{S1} has a minimum at about 10 GeV and q increases primitively and saturates at about 10 GeV is in agreement with recent work of Cleymans [53] in which the energy region $\sqrt{s_{NN}} \approx 10$ GeV for heavy-ion collisions is indicated to be an interesting one. In fact, in this energy region, the final state has the highest net baryon density, and a transition from a baryon dominated to a meson dominated final state takes place. At the same time, ratios of strange particles to mesons show obviously maxima in this energy region [53]. At a slightly smaller energy (about 6~8 GeV), other works show some extremes or saturation in excitation functions of parameters. These parameters include, but are not limited to, the specific reduced curvature of net-proton rapidity distribution [54–56], chemical freeze-out temperature [57, 58], mean transverse mass minus rest mass [57], yield ratios

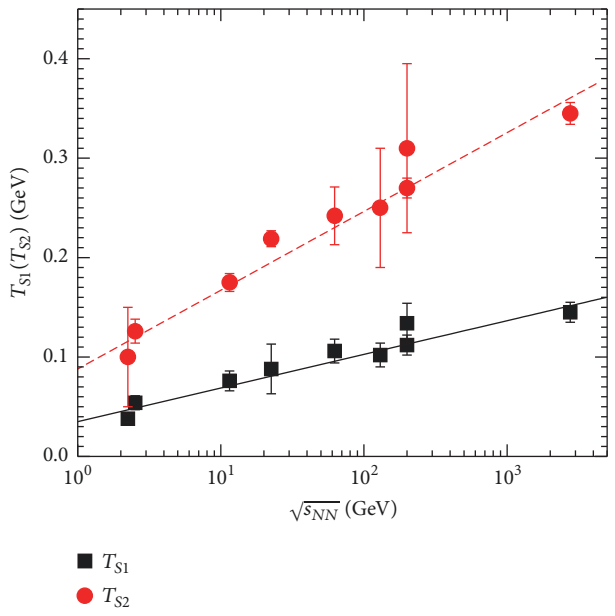

FIGURE 5: Dependence of T_{S1} (squares) and T_{S2} (circles) on $\sqrt{s_{NN}}$. The symbols represent the values of parameters taken from Table 1, and the error bars represent the statistical errors. The lines are the results fitted by the linear functions $T_{S1,S2} = a \ln \sqrt{s_{NN}} + b$.

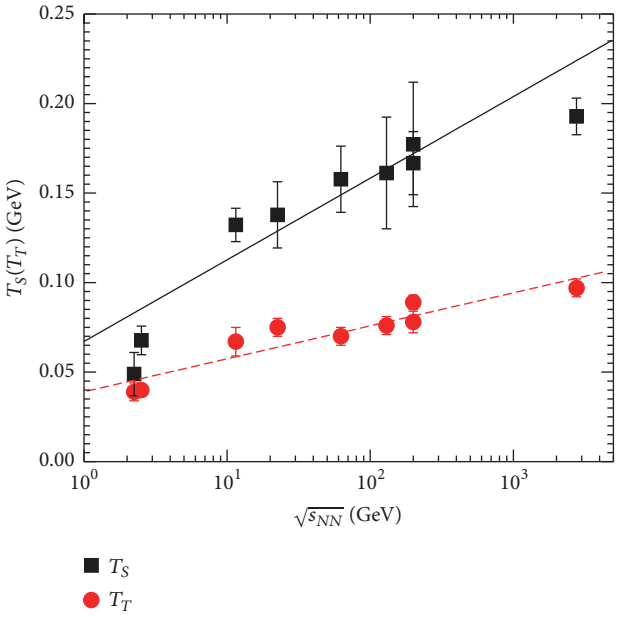

FIGURE 6: Same as Figure 5, but for the dependence of T_S (squares) and T_T (circles) on $\sqrt{s_{NN}}$ and the linear functions are $T_{S,T} = a \ln \sqrt{s_{NN}} + b$.

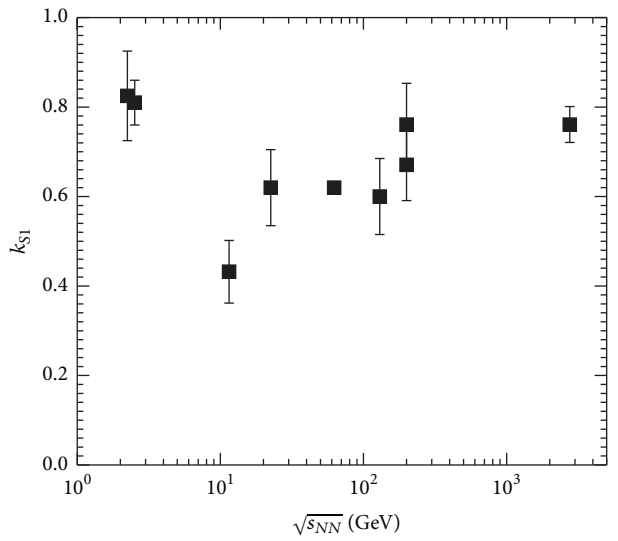

FIGURE 7: Dependence of k_{S1} on $\sqrt{s_{NN}}$. The symbols represent the values of parameter taken from Table 1 and the error bars represent the statistical errors.

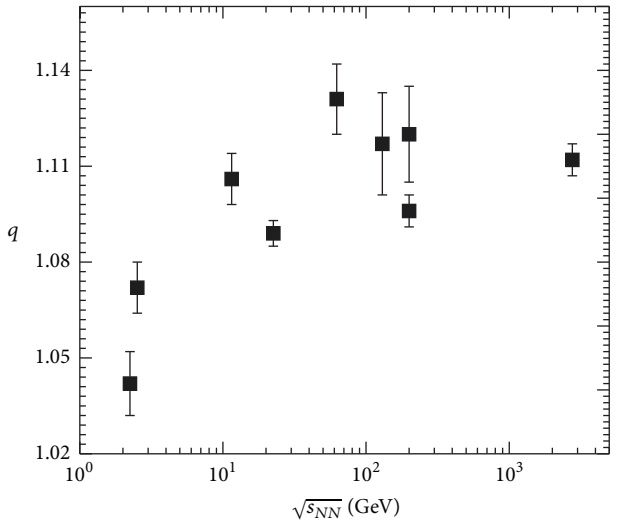

FIGURE 8: Dependence of q on $\sqrt{s_{NN}}$. The symbols represent the values of parameter taken from Table 1 and the error bars represent the statistical errors.

of positive kaons to pions [57–59], squared speed-of-sound [60], string tension in Schwinger mechanism [61], width and fraction of fragmentation source [62], and width ratios of experimental negative pion rapidity distribution to Landau hydrodynamic model prediction [58].

In the above analyses, for a not too wide transverse momentum spectrum, a standard distribution is usually not enough to describe the spectrum. Generally, we need a two-component standard distribution to describe the not too wide spectrum. It is expected that, in the case of studying a wider transverse momentum spectrum, we need a three-component standard distribution to describe the wider spectrum. If a set of experimental data is described by the two- or three-component standard distribution, it is also described by the Tsallis form of standard distribution [11]. If the two- or three-component standard distribution describes a temperature fluctuation between two or among three emission sources, the Tsallis form of standard distribution describes a degree of nonequilibrium. The degree of nonequilibrium is characterized by the entropy index q. A larger q corresponds to a farther nonequilibrium among different emission

sources. One can see from Table 1 that $q < 1.13$ in most cases, which renders an approximate equilibrium among different emission sources or the whole interacting system stays in an approximate equilibrium state.

Both the two- or three-component standard distribution and the Tsallis form of standard distribution describe only the results of soft excitation process. For the soft process, the particle spectrum appears with the characteristics of thermal emission phenomenon. Although the standard distribution describes the characteristics of thermal emission, some nonthermal emissions also obey the standard distribution. Even if the Tsallis form has less connection with thermal emission, they are relative due to the standard distribution. In the case of studying a very wide transverse momentum spectrum, for example, for a width of more than 5 GeV/c, to consider only the contribution of soft process is not enough in description of experimental data. To describe a wider transverse momentum spectrum, we have to consider simultaneously the contribution of hard scattering process. As mentioned in Section 2, according to the QCD calculus [18–20], the hard process can be described by the inverse power-law. Because of the hard process having no connection with the thermal emission, it does not affect the extraction of temperature parameter. In the case of extracting only temperature parameter, a too wide transverse momentum spectrum is not needed.

In the above analyses, the temperature extracted by us is in fact the effective temperature T. It is neither the temperature T_0 at the kinetic freeze-out nor the temperature $T_{\rm ch}$ at the chemical freeze-out of the emission source or interacting system. Generally, T_0 can be extracted from the transverse momentum spectra, and $T_{\rm ch}$ can be extracted from the ratios of different types of particles. However, the temperature extracted from the transverse momentum spectra is not surely T_0 due to the contribution of flow effect. How to get rid of the contribution of flow effect is a question that is worth discussing. In the blast-wave model [28–31], the mean transverse flow velocity $\langle\beta_T\rangle$ is introduced. Thus, T_0 and $\langle\beta_T\rangle$ can be simultaneously obtained based on the analysis of transverse momentum spectrum by the model. In addition, by using the standard distribution and its Tsallis form to analyze the transverse momentum spectra of different particles, we can obtain the linear relation between T and m_0. The intercept in the linear relation is regarded as T_0 [21, 29, 34–36]. We can also obtain the linear relation between $\langle p_T\rangle$ and mean moving mass $\overline{m}$ (mean energy). The slope in the linear relation is regarded as $\langle\beta_T\rangle$ [37–40].

Generally speaking, the two-component standard distribution and the Tsallis form of standard distribution are the same in essentials while differing in minor points in the behaviors in the figures. The standard distribution corresponds to the classical statistical system which has short-range interactions in interior and non-multifractal structure in boundary. Some extensive thermodynamic quantities such as energy, momentum, internal energy, and entropy are linearly related to the system size and particle number. These quantities obey simply additive property. The statistical method and the microscopic description of system are adaptive. The entropy function is a power tool to study the microscopic dynamics of system under the macroscopic condition by describing the occupation number of phase spaces of the system. The Tsallis form breaks through the limitation of classical statistics by using the entropy index q. The complex system with long-range interactions, local memory effect, strong dynamic correlation, fractal or multifractal occupation in phase space, and others can be described by the Tsallis form. The Tsallis form also causes the classical extensive quantities not to obey the simple additive property. Instead, the coupled item appears in the quantities and the nonextensive statistical effects are formed in the transverse and longitudinal dynamics [63–73].

In the above discussions, one can see that the two- or three-component standard distribution can be described by the Tsallis form of the standard distribution. It does not mean that the single standard distribution cannot be described by the Tsallis form. In fact, by using a lower temperature and an entropy index that is closer to 1, the Tsallis form describes well the single standard distribution. The standard distribution is successfully replaced by the Tsallis form due to q changing from 1 to a value that is greater than 1. This means that the interacting system changes from the classical and extensive statistical system to the nonextensive system, which is an essential change of the system properties. However, in some cases, the same set of experimental data can be described by both the (two- or three-component) standard distribution obeying the extensive statistics and the Tsallis form obeying the nonextensive statistics. This means that in these cases there is no obvious boundary to distinguish extensive system and nonextensive system for a given interacting system. We have to examine which property is the main factor. Or, the interacting system in the present energy range stays in a transition gradation from extensive system to nonextensive system.

4. Conclusions

We summarize here our main observations and conclusions.

(a) The transverse momentum spectra of negatively charged pions produced in central nucleus-nucleus collisions measured (simulated) in midrapidity range by different collaborations at the SIS, RHIC, and LHC are studied by the two-component standard distribution and the Tsallis form of standard distribution which are fitted into the frame of multisource thermal model. The two distributions describe approximately the experimental (simulated) data.

(b) The excitation functions of related parameters are analyzed. The four effective temperatures T_{S1}, T_{S2}, T_S, and T_T increase linearly with increase of $\ln\sqrt{s_{NN}}$. In particular, the relation between T_S and T_T can be obtained to be $T_S = (2.500 \pm 0.170)T_T + (-0.040 \pm 0.013)$ which shows a linear relation between T_S and T_T. With increase of $\sqrt{s_{NN}}$, k_{S1} has a minimum at about 10 GeV, and q increases primitively and saturates at about 10 GeV.

(c) There is no difference in the particle production in central nucleus-nucleus collisions from a few GeV to a few TeV. Combining with other works, one can say that the same or similar fits are good for proton-proton collisions. This suggests universality in particle production, as it is already

obtained in mean multiplicity, pseudorapidity density, and multiplicity distribution, but now for transverse momentum distribution as well.

(d) The energy of $\sqrt{s_{NN}} \approx 10$ GeV for heavy-ion collisions is indicated to have the highest net baryon density and the maximum ratios of strange particles to mesons and to take place a transition from the final state which has mainly baryons to the final state which has mainly mesons [53]. At a slightly smaller energy (about 6~8 GeV), other works show some extremes or saturation in excitation functions of some parameters [54–62]. These extremes and saturation are related to the search of soft point of equation of state.

(e) To be closer to the classical situation, the two- or three-component standard distribution has an advantage over the Tsallis form of standard distribution due to similar statistics for the classical situation and standard distribution. However, the Tsallis form of standard distribution uses less parameter than the two- or three-component standard distribution. If the two- or three-component standard distribution describes a temperature fluctuation between two or among three sources, the Tsallis form of standard distribution describes a degree of nonequilibrium.

(f) In the considered energy range, different emission sources stay in an approximate equilibrium state or the whole interacting system stays in an approximate equilibrium state. There is no obvious boundary to distinguish extensive system and nonextensive system for a given interacting system. The interacting system stays in a transition gradation from extensive system to nonextensive system. To obtain only the kinetic freeze-out temperature, we would rather use the two- or three-component standard distribution due to it being closer to the classical situation.

Conflicts of Interest

The authors declare that they have no conflicts of interest.

Acknowledgments

Comments on the manuscript and relevant communications from Edward K. G. Sarkisyan and Ya-Hui Chen are highly acknowledged. This work was supported by the National Natural Science Foundation of China under Grants nos. 11575103 and 11747319, the Shanxi Provincial Natural Science Foundation under Grant no. 201701D121005, and the Fund for Shanxi "1331 Project" Key Subjects Construction.

References

[1] E. K. G. Sarkisyan, A. N. Mishra, R. Sahoo, and A. S. Sakharov, "Multihadron production dynamics exploring the energy balance in hadronic and nuclear collisions," *Physical Review D*, vol. 93, no. 5, Article ID 054046, 2016.

[2] I. Bautista, J. G. Milhano, C. Pajares, and J. D. de Deus, "Multiplicity in pp and AA collisions: The same power law from energy-momentum constraints in string production," *Physics Letters B*, vol. 715, no. 1-3, pp. 230–233, 2012.

[3] Z. J. Jiang, Y. Zhang, H. L. Zhang, and H. P. Deng, "A description of the pseudorapidity distributions in heavy ion collisions at RHIC and LHC energies," *Nuclear Physics A*, vol. 941, pp. 188–200, 2015.

[4] G. Wolschin, "Ultraviolet energy dependence of particle production sources in relativistic heavy-ion collisions," *Physical Review C*, vol. 91, no. 1, Article ID 014905, 2015.

[5] M. Sanchis-Lozano and E. Sarkisyan-Grinbaum, "Ridge effect and three-particle correlations," *Physical Review D*, vol. 96, no. 7, Article ID 074012, 2017.

[6] F.-H. Liu, "Particle production in Au-Au collisions at RHIC energies," *Physics Letters B*, vol. 583, no. 1-2, pp. 68–72, 2004.

[7] F.-H. Liu, "Dependence of charged particle pseudorapidity distributions on centrality and energy in p(d)A collisions at high energies," *Physical Review C*, vol. 78, no. 1, Article ID 014902, 2008.

[8] F.-H. Liu, "Unified description of multiplicity distributions of final-state particles produced in collisions at high energies," *Nuclear Physics A*, vol. 810, no. 1–4, pp. 159–172, 2008.

[9] F.-H. Liu, "Charged particle production in d+Au collisions at $\sqrt{s_{NN}}$ = 200 GeV," *Physical Review C*, vol. 69, no. 6, Article ID 067901, 2004.

[10] S. Abreu, S. V. Akkelin, J. Alam et al., "Heavy-ion collisions at the LHC Last call for predictions," *Journal of Physics G*, vol. 35, no. 5, Article ID 054001, 2008.

[11] J. Cleymans and D. Worku, "Relativistic thermodynamics: transverse momentum distributions in high-energy physics," *The European Physical Journal A*, vol. 48, Article ID 160, 2012.

[12] A. N. Mishra, R. Sahoo, E. K. G. Sarkisyan, and A. S. Sakharov, "Effective-energy budget in multiparticle production in nuclear collisions," *The European Physical Journal C*, vol. 74, Article ID 3147, 2014.

[13] G. Wolschin, "Particle production sources at LHC energies," *Journal of Physics G: Nuclear and Particle Physics*, vol. 40, no. 4, Article ID 045104, 2013.

[14] I. Bautista, C. Pajares, J. G. Milhano, and J. D. De Deus, "Rapidity dependence of particle densities in pp and AA collisions," *Physical Review C*, vol. 86, no. 3, Article ID 034909, 2012.

[15] Z. J. Jiang and H. L. Zhang, "Pseudorapidity distributions of charged particles produced in p-p collisions at center-of-mass energies from 23.6 GeV to 900 GeV," *Modern Physics Letters A*, vol. 29, no. 27, Article ID 1450130, 2014.

[16] Z. J. Jiang, H. L. Zhang, J. Wang, and K. Ma, "The evolution-dominated hydrodynamic model and the pseudorapidity distributions in high energy physics," *Advances in High Energy Physics*, vol. 2014, Article ID 248360, 10 pages, 2014.

[17] H. Zheng and L. Zhu, "Comparing the Tsallis distribution with and without thermodynamical description in p+p collisions," *Advances in High Energy Physics*, vol. 2016, Article ID 9632126, 10 pages, 2016.

[18] R. Odorico, "Does a transverse energy trigger actually trigger on large-P_T jets?" *Physics Letters B*, vol. 118, no. 1-3, pp. 151–154, 1982.

[19] G. Arnison, A. Astbury, B. Aubert (UA1 Collaboration) et al., "Transverse momentum spectra for charged particles at the CERN proton-antiproton collider," *Physics Letters B*, vol. 118, no. 1-3, pp. 167–172, 1982.

[20] T. Mizoguchi, M. Biyajima, and N. Suzuki, "Analyses of whole transverse momentum distributions in $p\overline{p}$ and pp collisions by using a modified version of Hagedorn's formula," *International Journal of Modern Physics A*, vol. 32, no. 11, Article ID 1750057, 2017.

[21] S. Takeuchi, K. Murase, T. Hirano, P. Huovinen, and Y. Nara, "Effects of hadronic rescattering on multistrange hadrons in high-energy nuclear collisions," *Physical Review C*, vol. 92, no. 4, Article ID 044907, 2015.

[22] C. Gale, Y. Hidaka, S. Jeon et al., "Production and elliptic flow of dileptons and photons in a matrix model of the quark-gluon plasma," *Physical Review Letters*, vol. 114, no. 7, Article ID 072301, 2015.

[23] A. Andronic, P. Braun-Munzinger, and J. Stachel, "Thermal hadron production in relativistic nuclear collisions," *Acta Physica Polonica B*, vol. 40, pp. 1005–1012, 2009.

[24] A. Andronic, P. Braun-Munzinger, and J. Stachel, "The Horn, the hadron mass spectrum and the QCD phase diagram: the statistical model of hadron production in central nucleus-nucleus collisions," *Nuclear Physics A*, vol. 834, pp. 237c–240c, 2010.

[25] A. Andronic, P. Braun-Munzinger, and J. Stachel, "Hadron production in central nucleus-nucleus collisions at chemical freeze-out," *Nuclear Physics A*, vol. 772, no. 3-4, pp. 167–199, 2006.

[26] J. Cleymans, H. Oeschler, K. Redlich, and S. Wheaton, "Comparison of chemical freeze-out criteria in heavy-ion collisions," *Physical Review C*, vol. 73, no. 3, Article ID 034905, 2006.

[27] S. S. Adler, S. Afanasiev, C. Aidala (PHENIX Collaboration) et al., "Identified charged particles spectra and yields in Au+Au collisions at $\sqrt{s_{NN}}$ = 200 GeV," *Physical Review C*, vol. 69, Article ID 034909, 2004.

[28] E. Schnedermann, J. Sollfrank, and U. Heinz, "Thermal phenomenology of hadrons from 200A GeV S+S collisions," *Physical Review C*, vol. 48, no. 5, pp. 2462–2475, 1993.

[29] B. I. Abelev, M. M. Aggarwal, Z. Ahammed (STAR Collaboration) et al., "Systematic measurements of identified particles spectra in pp, d+Au, and Au+Au collisions at the STAR detector," *Physical Review C*, vol. 79, no. 3, Article ID 034909, 2009.

[30] B. I. Abelev, M. M. Aggarwal, Z. Ahammed (STAR Collaboration) et al., "Identified particle production, azimuthal anisotropy, and interferometry measurements in Au+Au collisions at $\sqrt{s_{NN}}$ = 9.2 GeV," *Physical Review C*, vol. 81, no. 2, Article ID 024911, 2010.

[31] Z. Tang, Y. Xu, L. Ruan, G. van Buren, F. Wang, and Z. Xu, "Spectra and radial flow in relativistic heavy ion collisions with Tsallis statistics in a blast-wave description," *Physical Review C*, vol. 79, no. 5, Article ID 051901, 2009.

[32] D. Thakur, S. Tripathy, P. Garg, R. Sahoo, and J. Cleymans, "Indication of a differential freeze-out in proton-proton and heavy-ion collisions at RHIC and LHC energies," *Advances in High Energy Physics*, vol. 2016, Article ID 4149352, 13 pages, 2016.

[33] T. Bhattacharyya, J. Cleymans, A. Khuntia, P. Pareek, and R. Sahoo, "Radial flow in non-extensive thermodynamics and study of particle spectra at LHC in the limit of small (q-1)," *The European Physical Journal A*, vol. 52, Article ID 30, 2016.

[34] H. Heiselberg and A.-M. Levy, "Elliptic flow and Hanbury-Brown-Twiss correlations in noncentral nuclear collisions," *Physical Review C*, vol. 59, no. 5, pp. 2716–2727, 1999.

[35] U. W. Heinz, Concepts of heavy-ion physics, Lecture Notes for Lectures Presented at the 2nd CERN-Latin-American School of High-Energy Physics, 1-14 June 2003, San Miguel Regla, Mexico, arXiv:hep-ph/0407360, 2004.

[36] R. Russo, *Measurement of D^+ meson production in p-Pb collisions with the ALICE detector [Ph.D. thesis]*, Universita degli Studi di Torino, Torino, Italy, 2015.

[37] H.-R. Wei, F.-H. Liu, and R. A. Lacey, "Kinetic freeze-out temperature and flow velocity extracted from transverse momentum spectra of final-state light flavor particles produced in collisions at RHIC and LHC," *The European Physical Journal A*, vol. 52, Article ID 102, 2016.

[38] H.-R. Wei, F.-H. Liu, and R. A. Lacey, "Disentangling random thermal motion of particles and collective expansion of source from transverse momentum spectra in high energy collisions," *Journal of Physics G: Nuclear and Particle Physics*, vol. 43, no. 12, Article ID 125102, 2016.

[39] H.-L. Lao, H.-R. Wei, F.-H. Liu, and R. A. Lacey, "An evidence of mass-dependent differential kinetic freeze-out scenario observed in Pb-Pb collisions at 2.76 TeV," *The European Physical Journal A*, vol. 52, Article ID 203, 2016.

[40] H.-L. Lao, F.-H. Liu, B.-C. Li, M.-Y. Duan, and R. A. Lacey, Examining the model dependence of extracting the kinetic freeze-out temperature and transverse flow velocity in small collision system, arXiv:1708.07749, 2017.

[41] W. Reisdorf, M. Stockmeier, A. Andronic (FOPI Collaboration) et al., "Systematics of pion emission in heavy ion collisions in the 1*A* GeV regime," *Nuclear Physics A*, vol. 781, no. 3-4, pp. 459–508, 2007.

[42] S. Das (for the STAR Collaboration), "Centrality dependence of freeze-out parameters from the beam energy scan at STAR," *Nuclear Physics A*, vol. 904–905, pp. 891c–894c, 2013.

[43] J. T. Mitchell (for the PHENIX Collaboration), "The PHENIX potential in the search for the QCD critical point, Talk given at the 3rd International Workshop on the Critical Point and Onset of Deconfinement, Florence, Italy, July 2006, arXiv:nucl-ex/0701079, 2006".

[44] M. Floris (for the ALICE Collaboration), "Identified particles in pp and Pb-Pb collisions at LHC energies with the ALICE detector," *Journal of Physics G: Nuclear and Particle Physics*, vol. 38, no. 12, Article ID 124025, 2011.

[45] C. Hartnack, R. K. Puri, J. Aichelin et al., "Modelling the many-body dynamics of heavy ion collisions: Present status and future perspective," *The European Physical Journal A*, vol. 1, pp. 151–169, 1998.

[46] J. Aichelin, "'Quantum' molecular dynamics–a dynamical microscopic n-body approach to investigate fragment formation and the nuclear equation of state in heavy ion collisions," *Physics Reports*, vol. 202, pp. 233–360, 1991.

[47] S. Das (for the STAR Collaboration), "Identified particle production and freeze-out properties in heavy-ion collisions at RHIC beam energy scan program," in *Proceedings of the EPJ Web of Conference*, vol. 90, Article ID 08007, 2015.

[48] E. K. G. Sarkisyan, A. N. Mishra, R. Sahoo, and A. S. Sakharov, "Centrality dependence of midrapidity density from GeV to TeV heavy-ion collisions in the effective-energy universality picture of hadroproduction," *Physical Review D*, vol. 94, no. 1, Article ID 011501, 2016.

[49] E. K. G. Sarkisyan and A. S. Sakharov, "Relating multihadron production in hadronic and nuclear collisions," *The European Physical Journal C*, vol. 70, no. 3, pp. 533–541, 2010.

[50] E. K. G. Sarkisyan and A. S. Sakharov, "On similarities of bulk observables in nuclear and particle collisions," in *Proceedings of the AIP Conference*, vol. 828, pp. 35–41, 2006.

[51] F.-H. Liu, Q.-W. Lü, B.-C. Li, and R. Bekmirzaev, "A description of the multiplicity distributions of nuclear fragments in hA and AA collisions at intermediate and high energies," *Chinese Journal of Physics*, vol. 49, pp. 601–620, 2011.

[52] F.-H. Liu, Y.-Q. Gao, T. Tian, and B.-C. Li, "Unified description of transverse momentum spectrums contributed by soft and hard processes in high-energy nuclear collisions," *The European Physical Journal A*, vol. 50, Article ID 94, 2014.

[53] J. Cleymans, The physics case for the $\sqrt{s_{NN}} \approx 10$ GeV energy region, arXiv:1711.02882 [hep-ph], 2017.

[54] Y. B. Ivanov and D. Blaschke, "Robustness of the baryon-stopping signal for the onset of deconfinement in relativistic heavy-ion collisions," *Physical Review C*, vol. 92, no. 2, Article ID 024916, 2015.

[55] Y. B. Ivanov, "Baryon stopping as a probe of deconfinement onset in relativistic heavy-ion collisions," *Physics Letters B*, vol. 721, no. 1-3, pp. 123–130, 2013.

[56] Y. B. Ivanov, "Alternative scenarios of relativistic heavy-ion collisions. I. Baryon stopping," *Physical Review C*, vol. 87, no. 6, Article ID 064904, 2013.

[57] L. Kumar (for the STAR Collaboration), "Identified hadron production from the RHIC beam energy scan," *Journal of Physics G: Nuclear and Particle Physics*, vol. 38, no. 12, Article ID 124145, 2011.

[58] A. Rustamov, "The horn, kink and step, dale: from few GeV to few TeV," *Central European Journal of Physics*, vol. 10, pp. 1267–1270, 2012.

[59] D. T. Larsen, "Energy dependence of hadron spectra and yields in p+p and ^{7}Be+^{9}Be collisions from the NA61/SHINE experiment at the CERN SPS," *Journal of Physics: Conference Series*, vol. 668, no. 1, Article ID 012020, 2016.

[60] F.-H. Liu, L.-N. Gao, and R. A. Lacey, "Searching for Minimum in Dependence of Squared Speed-of-Sound on Collision Energy," *Advances in High Energy Physics*, vol. 2016, Article ID 9467194, 9 pages, 2016.

[61] L.-N. Gao, F.-H. Liu, and R. A. Lacey, "Excitation functions of parameters in Erlang distribution, Schwinger mechanism, and Tsallis statistics in RHIC BES program," *The European Physical Journal A*, vol. 52, Article ID 137, 2016.

[62] L.-N. Gao, F.-H. Liu, Y. Sun, Z. Sun, and R. A. Lacey, "Excitation functions of parameters extracted from three-source (net-)proton rapidity distributions in Au-Au and Pb-Pb collisions over an energy range from AGS to RHIC," *The European Physical Journal A*, vol. 53, Article ID 61, 2017.

[63] C. Tsallis, "Possible generalization of Boltzmann-Gibbs statistics," *Journal of Statistical Physics*, vol. 52, no. 1-2, pp. 479–487, 1988.

[64] C. Tsallis and E. P. Borges, "Nonextensive statistical mechanics Applications to nuclear and high energy physics," in *Proceedings of the 10th International Workshop on Multiparticle Production*, N. Antoniou, Ed., 2003.

[65] W. M. Alberico, P. Czerski, A. Lavagno, M. Nardi, and V. Somá, "Signals of non-extensive statistical mechanics in high energy nuclear collisions," *Physica A: Statistical Mechanics and its Applications*, vol. 387, no. 2-3, pp. 467–475, 2008.

[66] C. Tsallis, "Nonadditive entropy: the concept and its use," *The European Physical Journal A*, vol. 40, pp. 257–266, 2009.

[67] G. Wilk and Z. Włodarczyk, "Power laws in elementary and heavy-ion collisions : a story of fluctuations and nonextensivity?" *The European Physical Journal A*, vol. 40, pp. 299–312, 2009.

[68] W. M. Alberico and A. Lavagno, "Non-extensive statistical effects in high-energy collisions," *The European Physical Journal A*, vol. 40, pp. 313–323, 2009.

[69] C. Tsallis, "An introduction to nonadditive entropies and a thermostatistical approach to inanimate and living matter," *Contemporary Physiscs*, vol. 55, no. 3, pp. 179–197, 2014.

[70] L. Marques, J. Cleymans, and A. Deppman, "Description of high-energy pp collisions using Tsallis thermodynamics: transverse momentum and rapidity distributions," *Physical Review D*, vol. 91, no. 5, Article ID 054025, 2015.

[71] C.-Y. Wong, G. Wilk, L. J. L. Cirto, and C. Tsallis, "From QCD-based hard-scattering to nonextensive statistical mechanical descriptions of transverse momentum spectra in high-energy pp and $p\overline{p}$ collisions," *Physical Review D*, vol. 91, no. 11, Article ID 114027, 2015.

[72] M. Rybczyński, G. Wilk, and Z. Włodarczyk, "System size dependence of the log-periodic oscillations of transverse momentum spectra," in *Proceedings of the EPJ Web of Conference*, vol. 90, 6 pages, 2015.

[73] H. Shababi and P. Pedram, "The minimal length uncertainty and the nonextensive thermodynamics," *International Journal of Theoretical Physics*, vol. 55, no. 6, pp. 2813–2823, 2016.